# Precursor of the Kondo resonance band in the heavy fermion system

Hong Chul Choi,[1,2] K. Haule,[3] G. Kotliar,[3] B. I. Min,[1,*] and J. H. Shim[1,2,4,†]

[1]*Department of Physics, Pohang University of Science and Technology, Pohang 790-784, Korea*
[2]*Department of Chemistry, Pohang University of Science and Technology, Pohang 790-784, Korea*
[3]*Department of Physics, Rutgers University, Piscataway, NJ 08854, USA*
[4]*Division of Advanced Nuclear Engineering, Pohang University of Science and Technology, Pohang 790-784, Korea*

(Dated: February 18, 2013)

We have investigated the formation of the Kondo resonance (KR) band and the hybridization gap (HG) in the heavy fermion compound $CeCoGe_2$, using a combined approach of the density functional theory (DFT) and the dynamical mean field theory (DMFT). Low temperature ($T$) spectral functions show dispersive KR states, similarly to the recent experimental observation. During the evolution from the *nonf* conduction band state at high $T$ to the dispersive KR band state at low $T$, which have topologically different band shapes, we have found the existence of kinks in the spectral function near $E_F$. The observation of kink is clearly in correspondence with the multiple temperature scale of the formation of the KR band. We suggest that the detailed analysis on the abrupt change of electron velocity and the scattering rate near the Fermi level will provide crucial information for the heavy fermion system.

PACS numbers: 71.20.-b, 71.27.+a, 75.30.Mb



In Ce-based heavy fermion compounds, the localized $4f$ and delocalized *nonf* (*spd*) states are orthogonal in the absence of the hybridization between them. Indeed, at high temperature ($T$), the energy levels of the localized $4f$ states are usually well separated from the Fermi level ($E_F$), and so only *nonf* dispersive conduction bands are observed near $E_F$ with the effectively small hybridization. At low $T$, however, the $4f$ states appear near $E_F$ and form the heavy quasiparticle bands hybridized with other conduction electrons. As a result of the hybridization, the effective mass of quasiparticles becomes tens to hundreds times larger than the bare electron mass. This quasiparticle band near $E_F$ can be identified as the dispersive Kondo resonance (KR) peak in the angle-resolved photoemission spectrum (ARPES).[1–3] The hybridization gap[4] (HG) is also induced below the coherent temperature ($T^*$), where the heavy quasiparticle bands begin to emerge.

The HG feature was directly observed by the optical conductivity,[5–10] and described theoretically by the periodic Anderson model.[4] The optical conductivities show the mid-infrared peaks in the energy range of several-tens meV at low $T$. These peaks are suppressed with increasing $T$ and disappear well above $T^*$ to produce the incoherent Drude peak at zero frequency. The magnitude of the HG ($\Delta_{HG}$) measures the hybridization strength between $f$ and other *nonf* conduction states. Recently, the dynamical mean field theory (DMFT) approach revealed the formation of the HG in $CeIrIn_5$ by calculating $T$-dependent spectral function $A(k,\omega)$.[11] The momentum-dependent $\Delta_{HG}$ at low $T$ was in good agreement with the measured spectrum and provided the information of the orbital-dependent hybridization strength.

In this letter, we have theoretically described the formation of the dispersive KR band and the HG in the heavy fermion compound $CeCoGe_2$.[12] The KR states are composed of dispersive bands arising from the hybridization of *nonf* and renormalized $f$ bands, and show quantitative agreement with the recent ARPES measurement.[2] We have shown that the formation of the KR band, which brings about a topological change of the band structures, should be accompanied by the kinks in the spectral function. We propose that the kink could appear in the *nonf* spectral function ($A^{nonf}(\mathbf{k},\omega)$) prior to the formation of the KR band around $T^*$.

The kink, the abrupt change in the band dispersion, is usually observed in the ARPES measurements of high $T_C$ superconductors.[13–17] The discontinuous quasiparticle band is induced by various collective excitations, such as phonon[13–15] and spin-fluctuation.[16] When the strong electron-phonon coupling disturbs the velocity and the scattering rate of electrons, ARPES spectrum[18–20] near the phonon energy shows the abrupt change in the slope of the energy-momentum dispersion. The ARPES experiment on $USb_2$ also revealed the kink feature in the dispersion of $f$ bands, which was explained by the combination of quasiparticle bands and many-body correction of the electron-spin-fluctuation coupling.[21] On the other hand, it was reported that the pure electronic correlation in the Hubbard model can produce such a kink near $E_F$,[22] which suggests that the one-particle picture should be strongly renormalized below a certain energy $\omega^*$ to have the kink feature in momentum space. Subsequent studies, however, showed that the kink in the Hubbard model arises from the internal spin-fluctuation mode.[23–25] In the present study, instead of kinks in correlated bands, we show that kinks can be phenomenologically observed in noncorrelated bands due to the formation of correlated $f$ states in the heavy fermion system.

We have used the density functional theory (DFT)+ DMFT method,[26] implemented in the linearized Muffin-Tin orbital band method.[27] We have considered the experimental crystal structure and the Brillouin zone shown in Fig. 1. The DMFT calculation considers only the local

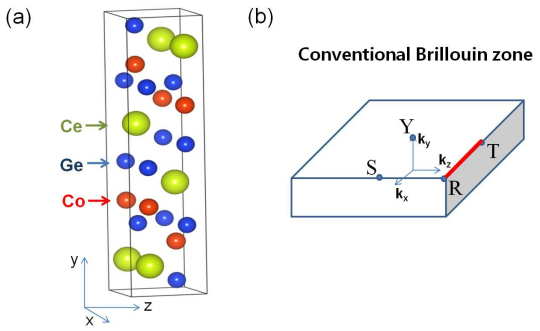


FIG. 1: (color online) Crystal structure and its Brillouin zone (a) The crystal structure of $CeCoGe_2$.[30] (b) The conventional Brillouin zone. Red line represents the path used in Fig. 3.

self-energy of $4f$ orbital, and other orbitals are considered in the DFT part. The local correlation effect is contained in the self-energy $\Sigma(\omega)$, which can be calculated from the corresponding impurity problem. To solve the impurity problem, we used a vertex corrected one-crossing approximation (OCA),[26] which is a self-consistent diagrammatic method perturbed in the atomic limit.[28] It has been checked that the OCA describes well the $T$-dependent spectral function of heavy fermion compound.[11,29] We neglected the crystalline electric field (CEF) effect on the local correlation energy because $CeCoGe_2$ has been confirmed as $j = 5/2$ heavy fermion.[12]

Figures 2(a) and 2(b) show $A^{nonf}(\mathbf{k},\omega)$'s along $S$-$R$-$T$-$Y$ at $T = 1200$ and 10 K, which demonstrates the formation of the KR bands near $E_F$. The dispersive *spd* bands at high $T$ (1200 K) look almost vertical due to the narrow energy range. At low $T$, as a result of the hybridization, new coherent quasiparticle bands are formed to give the different band geometry near $E_F$. For example, there are two separate bands crossing $E_F$ between $S$ and $R$ at high $T$, while, at low $T$, additional $j = 5/2$ bands with the bandwidth of ∼10 meV are introduced to produce degenerated three composite quasiparticle bands. As a result, the lower part of two bands observed at high $T$ are warped due to the hybridization, as indicated by green circle in Fig. 2(b). One band closer to $S$ is pushed down below $E_F$, but another band still intersects $E_F$. It is interesting that the formation of the parabolic-like hybridized band originated from high $T$ seperated bands below $E_F$ around $k$ = D at low $T$. All those features result in the change of geometry in the FS, as will be shown in Figs. 4(e) and 4(f).

$T$-dependent formation of the HG has been examined at the chosen $\mathbf{k}$-points in Figs. 2(c)-(f). At high $T$, $A^{nonf}(\mathbf{k},\omega)$ shows a general quasiparticle spectral feature with a single Gaussian function at each $k$-point. With lowering $T$, the spectral weights of $A^{nonf}(\mathbf{k},\omega)$ near $E_F$ begin to be transferred to upper and lower peaks separated by $\Delta_{HG}$ to form a gap structure. At low $T$, the clear gap can be observed at each chosen $\mathbf{k}$-point. The size of gap $\Delta_{HG}$ in $A^{nonf}(\mathbf{k},\omega)$ can be measured by the

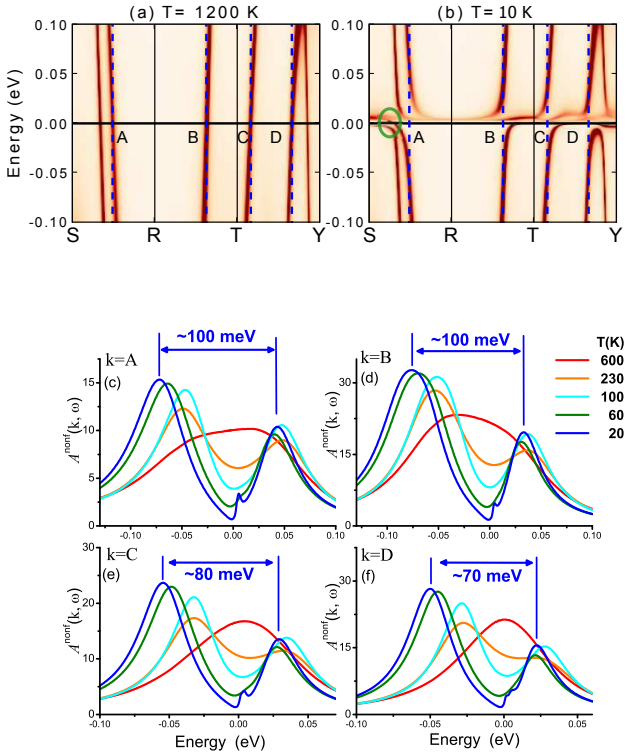


FIG. 2: (color online) Theoretical demonstration of the HG feature from $T$-dependent $A^{nonf}(\mathbf{k},\omega)$. $A^{nonf}(\mathbf{k},\omega)$'s are provided along $S$-$R$-$T$-$Y$ (a) at $T = 120$ K, and (b) at $T = 30$ K. $S$, $R$, $T$, and $Y$ are $\mathbf{k} = (\pi/2,\pi/2,0)$, $(\pi/2,\pi/2,\pi/2)$, $(0,\pi/2,\pi/2)$, and $(0,\pi/2,0)$, respectively. The green circle in (b) is for the emphasis of the $T$-dependent change. Blue dotted lines marked by A, B, C, and D represent $\mathbf{k}$-points, where the $T$-dependent $A^{nonf}(\mathbf{k},\omega)$ calculations in (c)-(f) are done. Theoretically predicted $\Delta_{HG}$ is given at each $\mathbf{k}$-point.

optical conductivity. Because $\Delta_{HG}$ has a variation of 70 ∼ 100 meV depending on $\mathbf{k}$-points, the measured $\Delta_{HG}$ should show multiplet structures or widespread shape in the optical conductivity measurements. The small peaks near $E_F$ at 20 K are induced due to the formation of quasiparticle bands of $j = 5/2$ states within the HG.

Figure 3 shows both $A^{nonf}(\mathbf{k},\omega)$ and the $f$ spectral function ($A^{f}(\mathbf{k},\omega)$) along $R$-$T$, and the integrated density of states (DOS) around $E_F$ at $T = 1200$, 300, and 10 K. The $T$-dependent development of the KR states is clearly confirmed in the DOSs of Figs. 3(c), (f), (i). At high $T$, the upper and lower Hubbard bands are located near $2 \sim 3$ eV above $E_F$ and 2 eV below $E_F$, respectively (not shown here). At the elevated $T$, the profile of the DOS near $E_F$ comes mostly from *nonf* states, although there is a weak background spectrum of $4f$ states. With lowering $T$, the weights of the upper and lower Hubbard bands are reduced and transferred to the KR states near

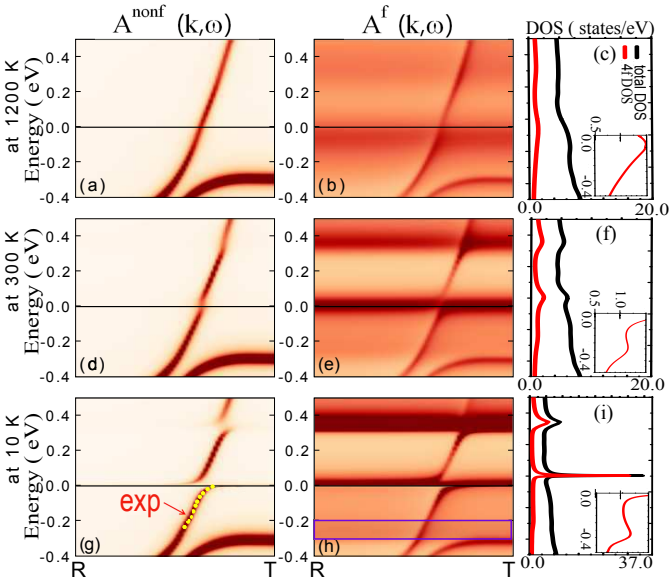


FIG. 3: (color online) $T$-dependent $A^{nonf}(\mathbf{k},\omega)$ ((a),(d),(g)) and $A^{f}(\mathbf{k},\omega)$ ((b),(e),(h)) between $R$ $(\pi/2,\pi/2,\pi/2)$ and $T$ $(0,\pi/2,\pi/2)$. The corresponding DOS's are also given in (c),(f), and (i). The inset shows the detail of the spin-orbit multiplet at $-300$ meV. Inside the purple rectangle in (h), the weak spectrum of spin-orbit multiplet is seen. Yellow points in (g) represent the off-resonant ARPES spectra in the measurement,[2] which are shifted along the **k**-path for better alignment of $nonf$ bands.

$E_F$. The $4f$ states give the main contribution to the DOS near $E_F$ below $T^*$.

At high $T$ (1200 K), $A^f(\mathbf{k},\omega)$ shows weak intensity near $E_F$, but has clear dispersive band feature similar to $A^{nonf}(\mathbf{k},\omega)$. This means that small hybridization still exists between $nonf$ and $f$ states at high $T$. The broad Gaussian peaks in $A^{nonf}(\mathbf{k},\omega)$ at high $T$, as shown in Figs. 2(c)-(f), are the indication of this hybridization. At low $T$ (10 K), where the KR states are fully developed, both $A^f(\mathbf{k},\omega)$ and $A^{nonf}(\mathbf{k},\omega)$ show the KR band structures with different weight distribution. The $nonf$-dominant bands form the gap structure with low intensity at $E_F$, while the $f$-dominant bands are confined near $E_F$ to give the sharp KR peak in the integrated DOS, as shown in Fig. 3(i). Note that the KR states should be considered as dispersive band structures, as described in the periodic Anderson model.

$A^{nonf}(\mathbf{k},\omega)$ and $A^f(\mathbf{k},\omega)$ at low $T$ (10 K) show good agreement with the off-resonance and on-resonance ARPES measurements at $T = 17$ K,[2] respectively. Especially, the momentum dependence of dispersive KR peaks in the experiments is well consistent with the calculated spectrum, as shown in Fig. 3(g). Also the weight distribution of $nonf$ and $f$ states observed in experiments are correctly captured in the calculation. The weak dispersion-less spin-orbit multiplet peak, which exists inside the purple rectangle in Fig. 3(h), is also consistent with the experimental observation. The spin-orbit multiplets of $A^f(\mathbf{k},\omega)$ are shown around $\pm 0.3$ eV, and their intensities increase as lowering $T$. Insets in Figs. 3(c), (f), (i) provide the $T$-dependent enhancement of the spin-orbit multiplet around $-0.3$ eV. It is noteworthy that the multiplet shows almost flat feature because the incoherent feature (broadening of bands) is much bigger than the dispersion of the KR states.

Because the spectra of high and low $T$ show clearly different quasiparticle band structures near $E_F$, the $T$-dependent evolution should show some phase transition. Figures 3(d) and (e) show the spectra in the intermediate $T$. $A^f(\mathbf{k},\omega)$ around $E_F$ shows effectively dispersion-less feature, which is the precursor of the formation of the KR states. Below and above the KR state, the $nonf$ bands are warped in different directions. At the energy of the KR state, the $nonf$ bands are not well defined due to the incoherent contribution of $A^f(\mathbf{k},\omega)$ to the $nonf$ states. As a result, $A^{nonf}(\mathbf{k},\omega)$ shows the feature of kinks near $E_F$. Distinctly from the kinks observed in other correlated systems, such as high $T_C$ superconductor, the kinks in heavy fermion system should appear in the noncorrelated bands during the formation of the KR bands and the HG.

Figures 4(a)-(d) show the schematic picture of emergence of kink during the formation of the KR bands (see the Supplementary Movie). At high $T$ in Fig. 4(a), there are only $nonf$ conduction bands that can be usually well described by the open-core band calculation, in which the occupied Ce $4f$ state is treated as a core level. With lowering $T$ in Fig. 4(b), the incoherent KR states of $4f$ electrons start to contribute to $E_F$, whereby the kink feature starts to emerge in $A^{nonf}(\mathbf{k},\omega)$. Here the kink structure is far from the "water-fall" shape, rather close to a "bell" shape. As decreasing $T$ further, the $f$ electrons start to be coherent slowly, and the $nonf$ bands are still being deformed. This process corresponds to Fig. 4(c), where the coherent character of bands becomes enhanced around $E_F$. In this case, $A^{nonf}(\mathbf{k},\omega)$ has the kink structure of the "water-fall" shape. At lower $T$ in Fig. 4(d), most $4f$ electrons near $E_F$ become coherent to make the fully coherent bands near $E_F$. Accordingly, the region of the kink feature is changed into that of the HG feature. Interestingly, the electron FS area gradually enlarges during this procedure.

The area of the electron FS around $R$, which is identified as $\alpha$ branch in Figs. 4(e) and (f), increases continuously with lowering $T$. In our recent DMFT study[29] on the FS of heavy fermion $CeIrIn_5$, two temperature scales are proposed: one ($T_f$) for the $T$-dependent evolution of the FS size, and the other ($T_m$) for the $T$-dependent evolution of the cyclotron effective mass ($m^*$). $T_f$ should be related to the contribution of local $4f$ electron to conduction electron. On the other hand, $T_m$ is a characteristic of the formation of coherent $4f$ bands in the lattice since the $m^*$ reflects the renormalization of the carriers. the

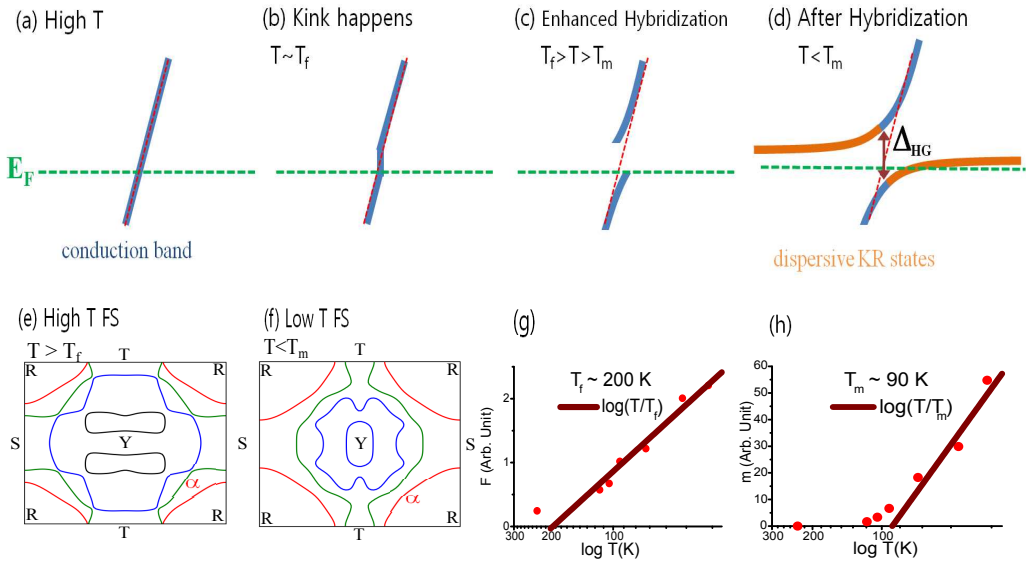


FIG. 4: (color online) The formation of the HG can be divided into four processes in (a)-(d), using $T_f$ and $T_m$ that are obtained by the scaling analysis in (g) and (h). (a) The high $T$ quasiparticle band is displayed. The blue color represents $A^{nonf}(\mathbf{k},\omega)$. (b) For $T \sim T_f$, the quasiparticle band is interrupted by the incoherent $4f$ electrons. The red dotted-line is provided as a guide for the high $T$ band. (c) For $T_f > T > T_m$, the hybridization between $nonf$ and $4f$ electrons is strengthened. (d) For $T < T_m$, the HG and $k$-dependent (dispersive) KR state can be well defined. The orange color represents $A^f(\mathbf{k},\omega)$. With lowering $T$, $E_F$ increases gradually due the participation of the new carrier from the incoherent $4f$ electrons. The FS on $\mathbf{k}$=Y plane at high and low $T$ are provided in (e) and (f), respectively. Color represents the different band indices. The scaling behaviors of $T$-dependent difference of the Fermi surface size (F) and the cyclotron effective mass ($m^*$) for the FS branch $\alpha$ shown in (e) and (f) are analyzed in (g) and (h), respectively.

same scaling behavior is also shown in $CeCoGe_2$. The FS branch $\alpha$, which is the well-defined FS branch at all $T$, as shown in Figs. 4(e) and (f), is chosen for this study. By analyzing $T$-dependent scaling behaviors in Figs. 4(g) and (h), we found $T_f \sim 200$ K and $T_m \sim 90$ K, respectively, for $\alpha$ branch.

The kink can be observed around $T_f$, where the incoherent $f$ state contributes to $E_F$. (see the Supplementary Movie.) The kink phenomenon is changed into the gap feature gradually between $T_f$ and $T_m$, where the contribution of incoherent $4f$ electron states disturb the band dispersion near $E_F$. Well below $T_m$, the HG and KR states are well defined. So, the formations of the kink around $T_f$ (200 K) will be the precursor of the HG below $T_m$ (90 K). Note that the kink features are also observed around 0.3 eV above $E_F$, as shown in Fig 3.(a), due to the incoherent contribution of spin-orbit multiplet. The multiplet around $-0.3$ eV does not give the kink because the contribution of $f$ state is too weak to distort the $nonf$ bands.

In summary, we have analyzed the $T$-dependent evolutions of $A(\mathbf{k},\omega)$ in the heavy fermion compound $CeCoGe_2$. It is shown that the DFT+DMFT calculations are consistent with the experimental measurements. We propose that the kink of $A^{nonf}(\mathbf{k},\omega)$ around $E_F$ can be identified during the evolution from the dispersive $nonf$ state at high $T$ to the HG and KR states at low $T$. Phenomenologically, the kinks observed in this work will show similar shape to those in other experiments, even though the conventional kinks appear in the correlated bands via the interaction with other excitations, such as phonon and spin-fluctuation. The kink induced by the correlation between the incoherent $4f$ and dispersive $nonf$ electrons above $T^*$ can be investigated in the state-of-the-art $T$-dependent ARPES experiments.

### Acknowledgments

We acknowledge useful discussions with H. Im and T. Park. This work was supported by the National Research Foundation of Korea(NRF) funded by the Ministry of Education, Science and Technology (No. 2009-007994, 2010-0006484, 2010-0026762, 2012029709).

## I. SUPPLEMENTARY INFORMATION

The images for moving picture (Movie) is provided for the additional Supplementary information. Movie shows the $T$-dependent variation of the $nonf$ spectral function $A(\mathbf{k},\omega)$.

* bimin@postech.ac.kr
† jhshim@postech.ac.kr

[1] J. W. Allen, J. Phys. Soc. Jpn. **74**, 34 (2005).
[2] H. J. Im, T. Ito, H-D. Kim, S. Kimura, K. E. Lee, J. B. Hong, Y. S. Kwon, A. Yasui, and H. Yamagami, Phys. Rev. Lett. **100**, 176402 (2008).
[3] M. Klein *et al.*, Phys. Rev. Lett. **106**, 186407 (2011).
[4] P. Coleman, arXiv:cond-mat/0206003.
[5] F. Marabelli and P. Wachter, Physica Scripta **T45**, 120 (1992).
[6] S. V. Dordevic, D. N. Basov, N. R. Dilley, E. D. Bauer and M. B. Maple, Phys. Rev. Lett. **86**, 684 (2001).
[7] C. I. Lee, K. E. Lee, Y. Y. Song, H. J. Im, S. Kimura, and Y. S. Kwon, Infrared Phys. Techn. **51**, 488 (2008).
[8] Y. S. Kwon, K. E. Lee, M. A. Jung, E. Y. Song, H. J. Oh, H. J. Im, and S. Kimura, Journal of Magnetism and Magnetic Material **310**, 310 (2007).
[9] S. Donovan, A. Schwartz, and G. Grüner, Phys. Rev. Lett. **79**, 1401 (1997).
[10] D. A. Bonn, J. D. Garrett, and T. Timusk, Phys. Rev. Lett. **61**, 1305 (1988).
[11] J. H. Shim, K. Haule, and G. Kotliar, Science **318**, 1615 (2007).
[12] E. D. Mun, B. K. Lee, Y. S. Kwon, and M. H. Jung, Phys. Rev. B **69**, 085113 (2004).
[13] A. Lanzara *et al.*, Nature **412** 501 (2001).
[14] G.-H Gweon *et al.*, Nature **430** 187 (2004).
[15] E. Schachinger, J. P. Carbotte, and T. Timusk, Europhys. Lett. **86** 67003 (2009).
[16] T. Dahm *et al.*, Nature Physics **5** 217 (2009).
[17] J. Hwang, T. Timusk, and G. D. Gu, Nature **427** 714 (2004).
[18] M. Hengsberger, D. Purdie, P. Segovia, M. Garnier, and Y. Baer, Phys. Rev. Lett. **83**, 592 (1999).
[19] T. Valla, A. V. Fedorov, P. D. Johnson, and S. L. Hulbert, Phys. Rev. Lett. **83**, 2085 (1999).
[20] Eli Rotenberg, J. Schaefer, and S. D. Kevan, Phys. Rev. Lett. **84**, 2925 (2000).
[21] T. Durakiewicz *et al.*, Europhysics Lett. **84**, 37003 (2008).
[22] K. Byczuk, M, Kollar, H. Held, Y.-F. Yang, I. A. Nekraov, Th. Pruschke, and D. Vollhardt Nature Physics **3** 168 (2007).
[23] A. Macridin, M. Jarrell, T. Maier, and D. J. Scalapino, Phys. Rev. Lett. **99**, 237001 (2007).
[24] S. Chakraborty, D. Galanakis, and P. Phillips, Phys. Rev. B **78**, 212504 (2008).
[25] C. Raas, P. Grete, and G. S. Uhrig, Phys. Rev. Lett. **102**, 076406 (2009).
[26] G. Kotliar *et al.*, Rev. Mod. Phys. **78**, 865 (2006).
[27] S. Y. Savrasov, Phys. Rev. B **54**, 16470 (1996).
[28] R. D. Cowan, The Theory of Atomic Structure and Spectra (Univ. California Press, Berkeley, 1981).
[29] Hong Chul Choi *et al.*, Phys. Rev. Lett. **108**, 016402 (2012).
[30] The structure is drawn by the VESTA package.
K. Momma and F. Izumi, "VESTA: a three-dimensional visualization system for electronic and structural analysis." J. Appl. Crystallogr., **41**, 653 (2008).
[31] H. J. Im *et al.*, arXiv:0904.1008 (2009).